Analysis of the applicability of multi-temporal full polarimetric airborne L-band SAR scattering to paddy rice field mapping

Taylor & Francis
Taylor & Francis Group

Check for updates

Analysis of the applicability of multi-temporal full polarimetric airborne L-band SAR scattering to paddy rice field mapping

Chinatsu Yonezawa[a] and Manzabu Watanabe[b]

[a]Graduate School of Agriculture Science, Tohoku University, Sendai, Japan; [b]School of Science and Engineering, Tokyo Denki University, Saitama, Japan

5

ABSTRACT

A Synthetic Aperture Radar (SAR) is an all-weather imaging system that is often used for mapping paddy rice fields and estimating the area. Fully polarimetric SAR is used to detect the microwave scattering property. In this study, a simple threshold analysis of fully polarimetric L-band SAR data was conducted to distinguish paddy rice fields from soybean and other fields. We analysed a set of ten airborne SAR L-band 2 (Pi-SAR-L2) images obtained during the paddy rice growing season (in June, August, and September) from 2012 to 2014 using polarimetric decomposition. Vector data for agricultural land use areas were overlaid on the analysed images and the mean value for each agricultural parcel computed. By quantitatively comparing our data with a reference dataset generated from optical sensor images, effective polarimetric parameters and the ideal observation season were revealed. Double bounce scattering and surface scattering component ratios, derived using a four-component decomposition algorithm, were key to extracting paddy rice fields when the plant stems are vertical with respect to the ground. The alpha angle was also an effective factor for extracting rice fields from an agricultural area. The data obtained during August show maximum agreement with the reference dataset of estimated paddy rice field areas.

10

15

20

25

1. Introduction

Crop monitoring is a major application of remote sensing. Rice is the primary cultivated crop in the Asian-monsoon region, and estimating the area under rice cultivation is important for managing food production. Synthetic Aperture Radar (SAR) makes it possible to observe the Earth's surface under all weather conditions; this is important because in the Asian-monsoon region the rice growing season corresponds to the rainy season. Thus, the application of SAR data for monitoring paddy fields during the rice growing season has been studied (Kurosu, Fujita, and Chiba 1995).

Fully polarimetric SAR can be used to detect the scattering mechanism of geographic areas (e.g., Durden, van Zyl, and Zebker 1989). Recently, many approaches that use fully polarimetric SAR observation systems for rice field observation have been developed. Oh

30

35

et al. (2009) used a ground-based polarimetric scatterometer to observe a flooded rice field via temporal changes in the backscattering coefficients of L- and C-band fully polarimetric data. Studies based on observations using airborne fully polarimetric SAR systems have been conducted. The unsupervised classification approach has also been applied to multi-frequency airborne fully polarimetric SAR data acquired from an agricultural area, with a crop classification accuracy greater than 84% being obtained (Hoekman, Vissers, and Tran 2011). Paddy rice field observations using multi-incidence angle and multi-polarimetric X-band (Arii et al. 2017) and L-band (Arii et al. 2018) airborne SAR have led to the construction of precise backscatter models. In addition to airborne SAR systems, fully polarimetric SAR data from spaceborne systems can also be used for monitoring agricultural areas. RADARSAT-2 is a C-band spaceborne SAR and the fully polarimetric data that it has pulled from agricultural fields have been analysed to classify crop types (Jiao et al. 2014), to assess the phenological stage of rice fields (Lopez-Sanchez et al. 2014), and to estimate the aboveground biomass of oilseed (Yang et al. 2018). The usefulness of RADARSAT-2's decomposition parameters for rice field classification and monitoring has also been demonstrated, with a temporal change in the double bounce scattering component associated with paddy rice growth also figuring prominently (Li et al. 2012; Yonezawa et al. 2012). Further, a relationship has also been established between hybrid polarimetric parameters from the RADARSAT-2 data and the biophysical parameters of rice crop (Xie et al. 2015). In addition to C-band SAR, the potential for use of L-band fully polarimetric SAR in paddy rice field monitoring has also been reported (McNairn et al. 2009; Muthukumarasamy, Shanmugam, and Kolanuvada 2017). Compared to L-band SAR data analysis, C-band SAR data analysis results show a smaller percentage change in the double bounce scattering component ratio for mature rice fields (Yonezawa and Watanabe 2015). A small amount of time series data exists in the fully polarimetric datasets acquired by spaceborne L-band SAR during the rice growing season. This is because the ALOS PALSAR was only capable of fully polarimetric observation in experimental mode (Rosenqvist et al. 2001). Its successor sensor, PALSAR-2, mounted on ALOS-2, only allows for fully polarimetric observations approximately once per year in the ALOS-2 observation scenario.

For practical use of remote sensing data for crop field extraction and monitoring, it is important to map the target fields and estimate the area. Yonezawa (2017) showed that paddy rice fields can be distinguished from the surrounding agricultural land using polarimetric decomposition parameters derived from ALOS-2 PALSAR-2 images obtained during the rice well-growing season in early September. Yonezawa (2018) subsequently analysed PALSAR-2 data obtained during early August and examined the applicability of the same method to images from early August, corresponding to the rice heading season in the previous study. In this study, we investigated the possibility of paddy rice field extraction and mapping via simple threshold analysis of a single fully polarimetric SAR observation. We examined a set of ten airborne SAR L-band 2 (Pi-SAR-L2) images acquired during the growing seasons (June, August, and September) of 2012, 2013, and 2014. The observation periods corresponded to the pre-panicle development, heading, and well-growing stages of rice. Vector data for agricultural land use areas were overlaid on polarimetric decomposition images and the mean value used for paddy rice field extraction. Then, reference maps generated by optical sensor images obtained during flooding and heading in paddy rice fields were used to evaluate the data.

2. Study area and data analysis

2.1. Study area

Agricultural fields in the Wakabayashi ward of the city of Sendai in Japan were studied (Figure 1). The area comprising these fields was heavily damaged by the tsunami that followed the 2011 Great East Japan Earthquake. Sections of the damaged fields have been reconstructed each year since the earthquake occurred. Rice planting restarted east of the highway in 2012 (the year following the tsunami damage).

The main crops grown in this region are rice paddy and soybeans. This typifies the introduction of crop diversification into paddy fields in Japan, in which soybean is the major crop used for the purpose. The dates for the. start of transplanting and the heading stage, and the full heading date for rice paddy from 2012 to 2014 are shown in Table 1. Field surveys were conducted several times per year, concurrent with the observation periods of Pi-SAR-L2. Figure 2 shows photographs of a paddy rice field in the middle of June, the beginning of August, and the beginning of September, corresponding to Pi-SAR-L2 observations. A considerable portion of the field areas was covered by grass or bare soil because of land consolidation, which is carried out on different agricultural parcels each year.

2.2. Pi-sar-l data and data analysis

Fully polarimetric Pi-SAR-L2 data obtained in mid-June, mid-August, and mid-September in 2012, 2013, and 2014 were analysed (Table 1). Pi-SAR-L2 was developed by the Japan Aerospace Exploration Agency (JAXA) (Shimada et al. 2013a). Flight direction was
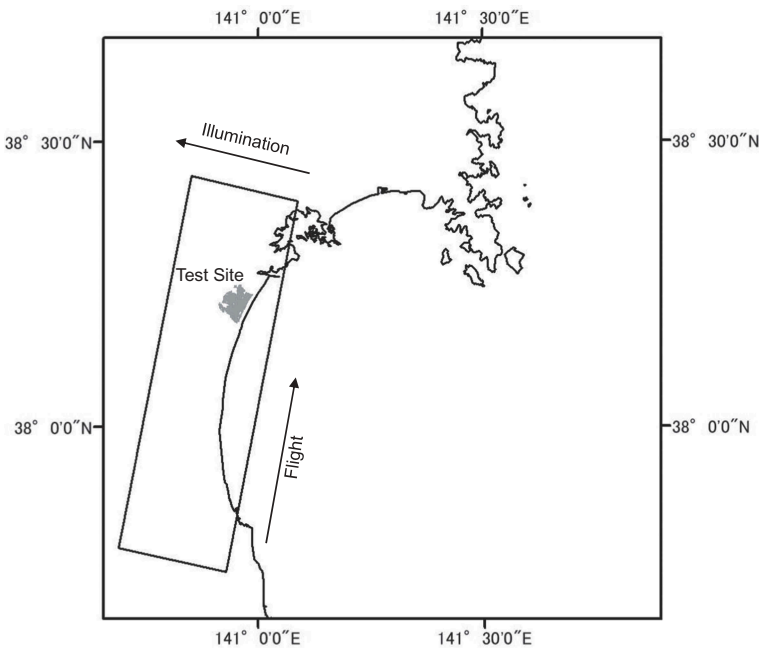

Figure 1. Test site. The square corresponds to the observation area of the Pi-SAR-L2 flight on 19 June 2012. The target agricultural field is shown in grey.

Table 1. Paddy rice growth stages, observation date for analysed Pi-SAR-L2 data and optical sensor data used in generating reference rice distribution map from 2012 to 2014.

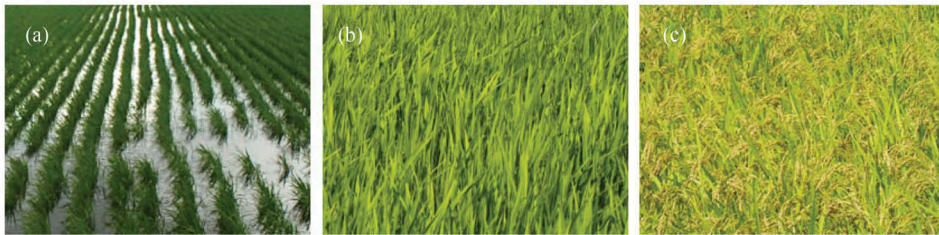|		2012	2013	2014
Paddy rice growth stage	Transplanting start	↓ 4 May	↓ 3 May	↓ 3 May
	Start of heading stage	↓ 4 Aug.	↓ 5 Aug.	↓ 30 Jul.
	Full heading	↓ 14 Aug.	↓ 16 Aug.	↓ 11 Aug.
Obs. date of Pi-SAR-L2		↓ 19 Jun.	↓ 10, 11 Jun.	↓ 12 Jun.
		↓ 10 Aug.	↓ 8 Aug.	↓ 6 Aug.
		↓ 10 Sep.	↓ 11 Sep.	↓ 11 Sep.
Obs. Date of Optical sensor	Landsat 7/ETM*	↓ 2 Jun.	↓ 5 Jun.	↓ 31 May
	Landsat 8/OLI*			↓ 3 Aug.
	Terra/ASTER**	↓ 21 Aug.	↓ 16 Aug.	

* Resolution 30m
** Resolution 15m

Figure 2. Paddy rice fields at the test site in (a) mid- June, (b) beginning of August, and (c) beginning of September.

approximately south to north and the incidence angle on the study area was approximately 30–45° for all observation data. Azimuth and slant range resolution of Pi-SAR-L2 is 0.8 m and 1.76 m, respectively (Shimada et al. 2013b).

Single-look complex data were analysed using PolSARpro software (Pottier and Ferro-Famil 2012). Four-component decompositions (Yamaguchi et al. 2005) were carried out with a 3 × 3 window size after deriving a 3 × 3 complex coherency matrix from the original data. The four-component decomposition model describes scattering contributions from double bounce, volume, surface, and helix scattering by using phase and intensity information obtained from polarimetric SAR data. We also attempted eigenvalue analysis of the coherency matrix. Eigenvalue-eigenvector decomposition (Cloude and Pottier 1996, 1997) was performed and the scattering entropy, polarimetric anisotropy, and alpha angle were computed. Polarimetric entropy describes the randomness of the scattering, polarimetric anisotropy is used to characterize the scattering phenomenon, and the alpha angle yields direct information about the scattering mechanism represented by each eigenvector. Following the decomposition analyses, the resulting images were projected onto a map with UTM coordinates for quantitative analysis of the agricultural parcel units and comparison with ground truth data.

Vector data for agricultural parcels were overlaid on the polarimetric decomposition results to validate the polarimetric decomposition data. In this study, an agricultural parcel vector dataset produced before the 2011 earthquake was modified to reflect the reconstruction after the tsunami damage based on the high-resolution optical sensor images. There are 9461 agricultural parcels in the 2014 dataset, comprising a total area of 1573 ha. This dataset was then overlaid on the analysed images and the mean values of the decomposition parameters for each agricultural parcel computed. The relative contribution of each scattering mechanism obtained from the four-component decomposition analysis was then investigated and the scattering component percentage for each scattering mechanism computed for each agricultural parcel.

2.3. Reference map generation from optical sensor images

To evaluate the PALSAR-2 data analysis results, optical sensor images obtained late May to early June and early to late August in 2012, 2013, and 2014 were used to generate reference paddy rice field maps (Table 1). The rice field flooding season is in late May and early June while the rice heading season is in August. The short-wavelength infrared

(SWIR) spectral band is used to identify increased water absorption in agricultural areas (Weichelt et al. 1991). Agricultural parcels in our dataset with a mean SWIR spectral band value less than a threshold value during the rice field flooding season were candidates for identification as paddy rice fields.

Actual rice fields were identified using the Normalized Difference Vegetation Index (NDVI) for the rice well-growing season (Osawa, Kunii, and Saito 2010). Within the agricultural parcels identified as paddy rice fields using the SWIR spectral band, a parcel with a mean NDVI greater than a threshold value was categorized as a paddy rice field, and others were categorized as soybean or other crop fields, including grasslands. The threshold values for the SWIR spectral band and NDVI were determined using the method described by Otsu (1979); these are shown in Table 2.

3. Results and discussion

3.1. Visual interpretation of paddy rice field distribution

Figure 3 shows the reference map of the distribution of paddy field agricultural parcels for 2012, 2013, and 2014. Note that in 2012, the paddy rice fields are distributed only to the east of the highway, which is represented by a black coloured strip running through the middle of Figure 3 (a). In 2013, the paddy rice fields are to the west of the highway. To the east of the highway, restart of paddy rice growth is confirmed in several fields neighbouring the highway; however, no paddy fields are found near the coastline. Until 2014, no paddy rice cropping was observed in agricultural fields located within 1 km from the coastline. The field survey results and the visual interpretations of the optical sensor data are consistent with the paddy rice field distribution determined using optical sensor data analysis. The agricultural parcel counts and areas of paddy rice and soybean and other fields categorized via optical sensor image analysis are shown in Table 3. Paddy rice fields occupied less than half of both the total count and the area in 2012, but increased to more than 50% of the total count and more than 60% of the total area in 2013. In 2014, paddy rice fields decreased by 2% in number and 1% in area from 2013 levels. This decrease was caused by land reconstruction and crop conversion from rice to soybeans.

Figure 4 shows the distribution of the double bounce scattering component percentage for the analysed Pi-SAR-L2 data. The difference between the areas of paddy rice field and that of soybean and other crops is unclear in the June data for all years. However, an increased double bounce scattering ratio for paddy rice field parcels is found in the August and September data. By visually comparing the double bounce scattering component percentage map with the reference map, the large percentage double bounce scattering component area for August and September data is found to correspond with

Table 2. Threshold values for The short-wavelength infrared (SWIR) spectral band and Normalized difference vegetation index (NDVI) used with optical sensor images to extract paddy rice fields.

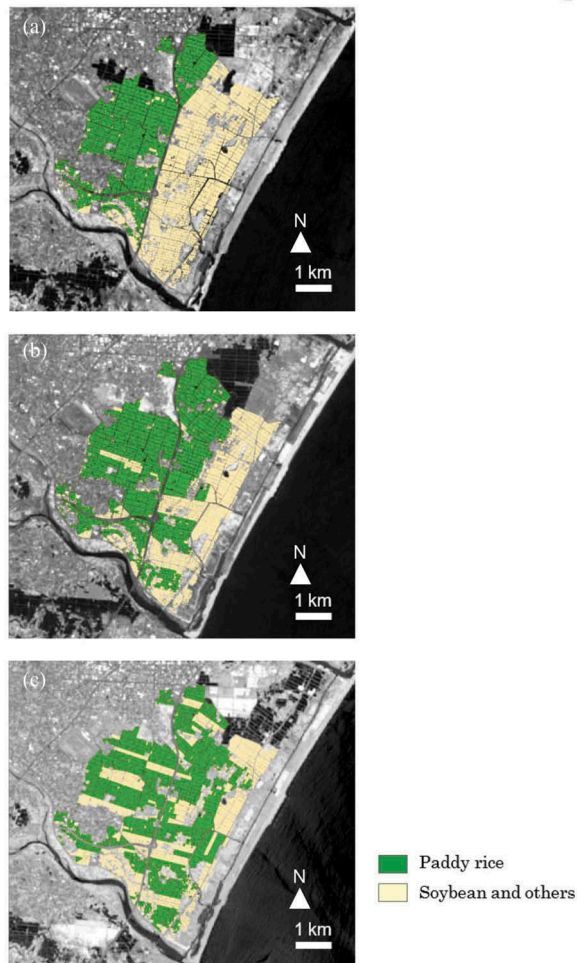| Year	SWIR threshold value (nm) (Late May or beginning of June)	NDVI threshold value (Early to mid-August)
2012	1526	0.300
2013	1720	0.520
2014	1573	0.541

COLOUR
FIGURE

Figure 3. Results of paddy rice parcel extraction during the rice field flooding season using the SWIR spectral band and NDVI determination during the rice well-growing season with SWIR images for (a) 2012, (b) 2013, and (c) 2014.

Table 3. Numbers and areas of paddy rice, soybean, and other crops derived from analyses of optical sensor data collected from late May through August of each year.

Year	Number of parcels		Area of parcels	
	Paddy rice	Soybean and others	Paddy rice (ha)	Soybean and others (ha)
2012	3727	5734	684.7	888.7
2013	5043	4418	968.9	604.4
2014	4803	4658	956.6	616.7

paddy rice field area for every year. A quantitative evaluation of these data is presented in section 3.3.

The distribution maps of the surface scattering component and alpha angle obtained from August and September observation data show possibilities for distinguishing between paddy rice fields and soybean and other crop fields. However, it is difficult to
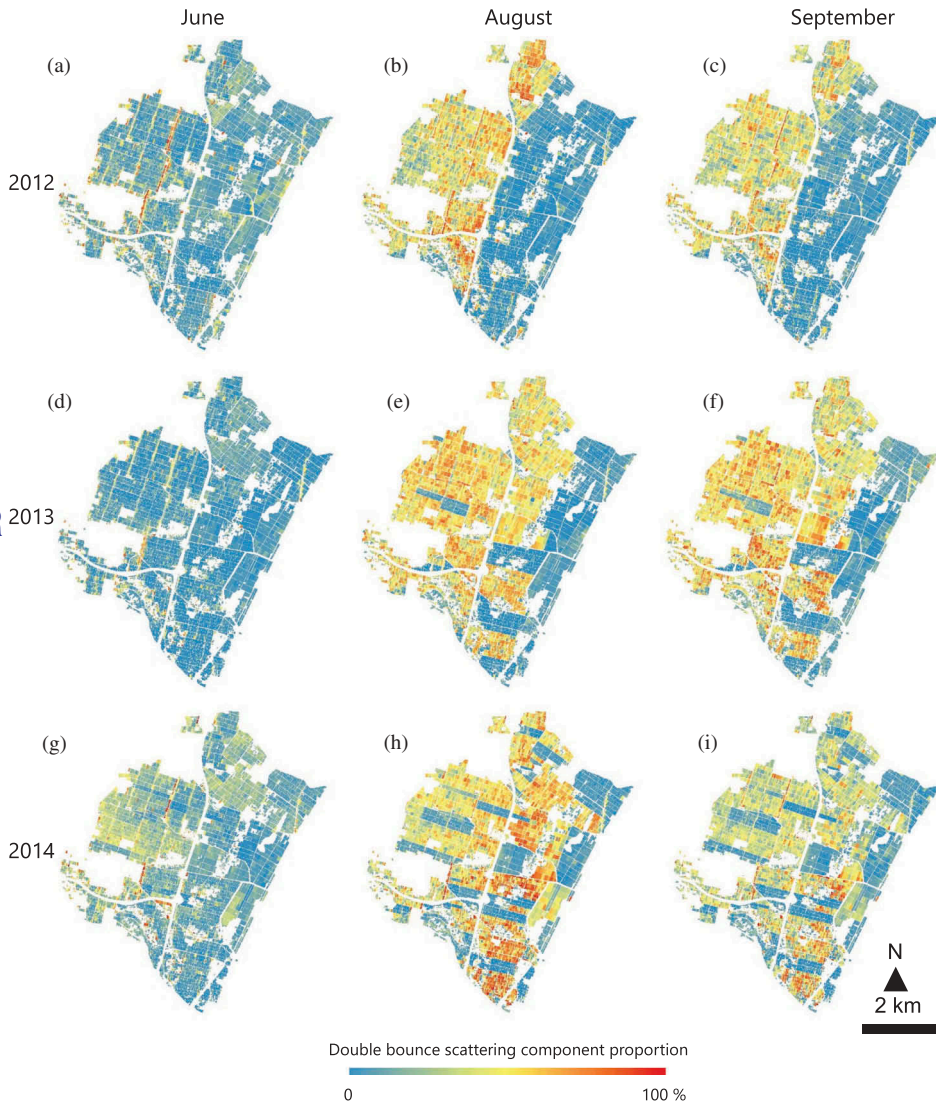
COLOUR
FIGURE

Figure 4. Distribution map of the double bounce scattering component percentage of Pi-SAR-L2 data based on agricultural parcels. (a) 19 June 2012, (b) 10 August 2012, (c) 10 September 2012, (d) 10 June 2013, (e) 8 August 2013, (f) 11 September 2013, (g) 12 June 2014, (h) 6 August 2014, and (i) 11 September 2014.

find notable differences in the June data. Figures 5 and 6 show the percentages of surface scattering component and alpha angle for each agricultural parcel in August 2012, 2013, and 2014. The distribution of the alpha angle in the September observation data is similar to that in the August observation data for all three years. The difference between paddy rice field and soybean and other crop fields appears in the August and September observations as a decrease in the percentage of paddy rice field parcels classified by optical sensor data analysis. Alpha angles of paddy rice field parcels increase from June to August; However, there is little change in the angles of soybean and other crop fields.
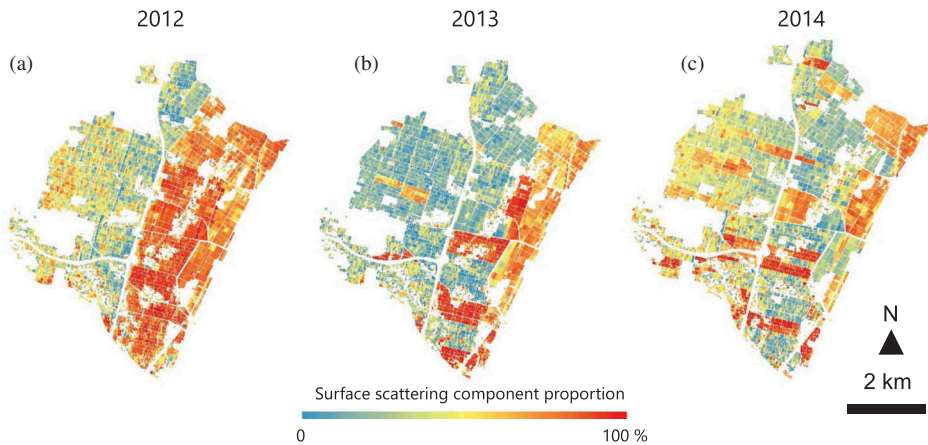
180

185

Figure 5. Distribution map for the surface scattering component percentage of Pi-SAR-L2 data, constructed based on agricultural parcels. (a) 10 August 2012, (b) 8 August 2013, and (c) 6 August 2014.
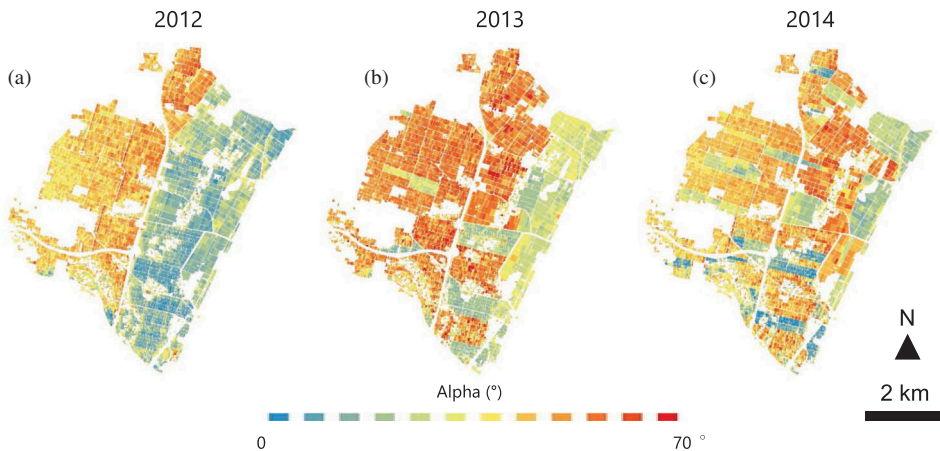

Figure 6. Distribution map of the alpha angle of Pi-SAR-L2 data based on agricultural parcels. (a) 10 August 2012, (b) 8 August 2013, and (c) 6 August 2014.

Figure 7 shows the distribution of the percentage of the volume scattering component in August 2012, 2013, and 2014. The volume scattering component is less than 50% for most agricultural parcels, and the difference dependent on crop type is not notable. Thus, we determined that it is difficult to distinguish paddy field agricultural parcels using the volume scattering component ratio or other decomposition parameters when considering data obtained during the observation period in this study.

These results can be explained by the effect of overall crop structure on the scattering mechanism. Paddy rice is in its growing stage, with a height of approximately 40 cm, in mid-June. At that time, flooding water can also be seen from above the field (Figure 2(a)). The difference in crop structure between paddy rice, soybean, and others becomes obvious in August. Paddy rice is now in the heading stage and its crop height is in the range 80–90 cm (Figure 2(b)). Double bounce scattering is caused by vertical pole
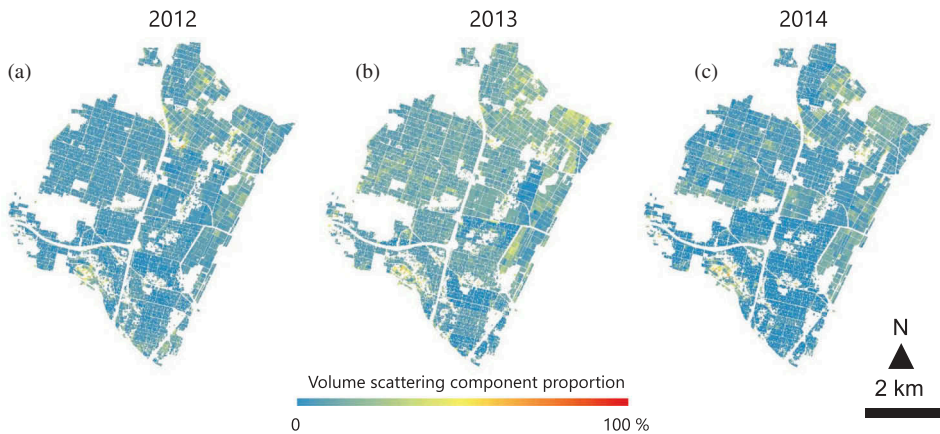
COLOUR
FIGURE

Figure 7. Distribution map of the volume scattering component percentage of Pi-SAR-L2 data based on agricultural parcels. (a) 10 August 2012, (b) 8 August 2013 and (c) 6 August 2014.

structures on the ground, and the paddy rice structure at this growth stage satisfies this vertical pole condition. Further, L-band SAR can penetrate thin paddy rice leaves, thereby causing double bounce scattering to dominate. In contrast, surface scattering is still dominant in the soybean and other crop fields, including grassland, in the test site at this time.

The alpha angle is related to the mean scattering process occurring, with 45° signifying a dipole. An alpha angle larger than 40° is found for the areas in the August observation data that correspond to the paddy rice fields on the reference map. Strong double bounce scattering, where the alpha angle is 90°, contributes to the larger alpha angle observed in August. The effect of the structural difference between the paddy rice, soybean, and others on the volume scattering component ratio in the case of L-band SAR is low.

An expanded view of a section of Figure 4(h) is presented in Figure 8. The distribution of the double bounce scattering component ratio in the paddy rice field area ranges from approximately 25 to more than 95%. One possibility for this range is Bragg scattering. Ouchi et al. (2006) and Arii et al. (2018) pointed out that the Bragg scattering effect enhances double-bounce scattering in rice plants observation using L-band SAR. The effect of Bragg scattering on the paddy rice fields, which differs by area, may therefore be included in the analysis results. However, for the discrimination of paddy rice fields from other crops, the enhancement resulting from double bounce scattering is advantageous.

3.2. Relationship between paddy field structure and the scattering mechanism

Figure 9 shows the temporal change in the mean value of the double bounce, surface scattering component ratio, and alpha angle for paddy rice agricultural parcels extracted from the optical sensor data analysis results. The number of days from paddy rice transplanting day to SAR data acquisition day was counted from respective start dates of 4 May 2012, 3 May 2013, and 3 May 2014. Values from the data collected on 11 June 2013 are plotted and are similar to values from data collected on 10 June 2013. Polarimetric

COLOUR
FIGURE

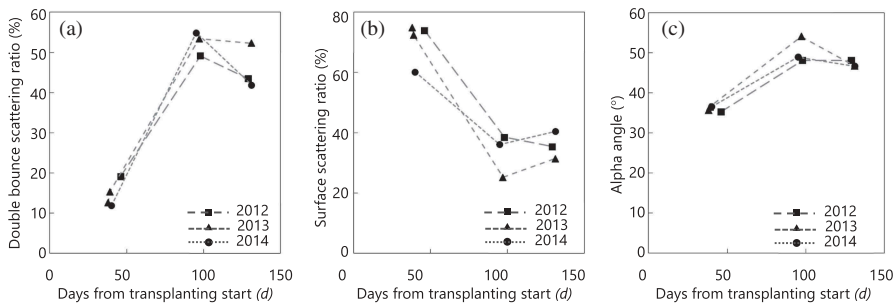**Figure 8.** Expanded view of a section of Figure 4(h).

COLOUR
FIGURE

Figure 9. Temporal change in polarimetric decomposition components, derived from ratio, (b) surface scattering component ratio, optical sensor data analysis of paddy rice field areas. (a) Double bounce scattering componentand (c) alpha angle.

decomposition components show a similar temporal change pattern for every year. The double bounce scattering component ratio reached its highest value, about 50%, in early August and decreased in early September. The surface scattering component ratio exhibited the opposite behaviour: its lowest value occurred in early August and the value then slightly increased in early September, with the exception of 2012. In 2012, the surface scattering component ratio decreased in early September. The mean alpha angle was 35-36° in June, increased to more than 45° in early August, and stayed above 45° in early September in all years.

Dominance of the surface scattering component because of the flooding water in mid-June appeared quantitatively. In August, the dominant scattering component is double bounce resulting from the vertical pole structure of the paddy rice. At the beginning of September, paddy rice is growing well and its structure is still vertical with respect to the

ground; however, the double bounce scattering ratio decreases marginally from August to September (Figure 9(a)). This decrease can be attributed to the tilting of the paddy rice stems as they mature (Figure 2(c)), which appears to change the scattering mechanism. The alpha angle is also sensitive to the tilting of the paddy rice stems.

A fully polarimetric SAR dataset obtained during the rice growing season has the potential to allow the extraction of paddy rice fields from among other crop fields. Data obtained in August show better agreement compared to the data obtained in September. This is explained by the fact that rice crops stand perpendicular to the ground in this area in early August. The secondary crop in this area is soybeans and it features are different from those of paddy. The site used in this study is a good location for paddy rice field extraction because it is flat and the paddy rice transplanting season occurs on almost the same date annually. Applying our method to another area is the next step for this research, and it is necessary to evaluate the possibility of separating paddy rice from corn or other vertically standing crops.

3.3. Paddy rice field extraction using threshold analysis

The ability to distinguish paddy rice fields from those of other crops using a simple threshold analysis of single fully polarimetric SAR data was also examined in this study. Otsu's (1979) method was applied to determine the threshold value for each mean polarimetric decomposition component of the agricultural parcels. Table 4 shows the determined threshold values. The cross-tabulation of classification results using the optical sensor data and the polarimetric decomposition parameters shows a clear availability of polarimetric SAR data for paddy rice field extraction.

Figures 10–12 show charts based on these cross-tabulations. The percentages of paddy rice and soybean and other field areas are shown by grey bars on the categories of optical sensor classification. The examined parameters are double bounce and surface scattering component percentages, and the alpha angle. We show quantitatively that, for the June data, a large percentage of the parcels are classified as soybean and other fields by all the examined parameters' analyses methods. In addition, paddy rice fields show higher estimation agreement rates than soybean and other crops in the collected data.

Table 4. Threshold values used to extract paddy rice fields determined by Otsu's method (Otsu 1979) for each mean polarimetric decomposition component. Dbl. and Odd refer to double bounce scattering and surface scattering components, respectively.

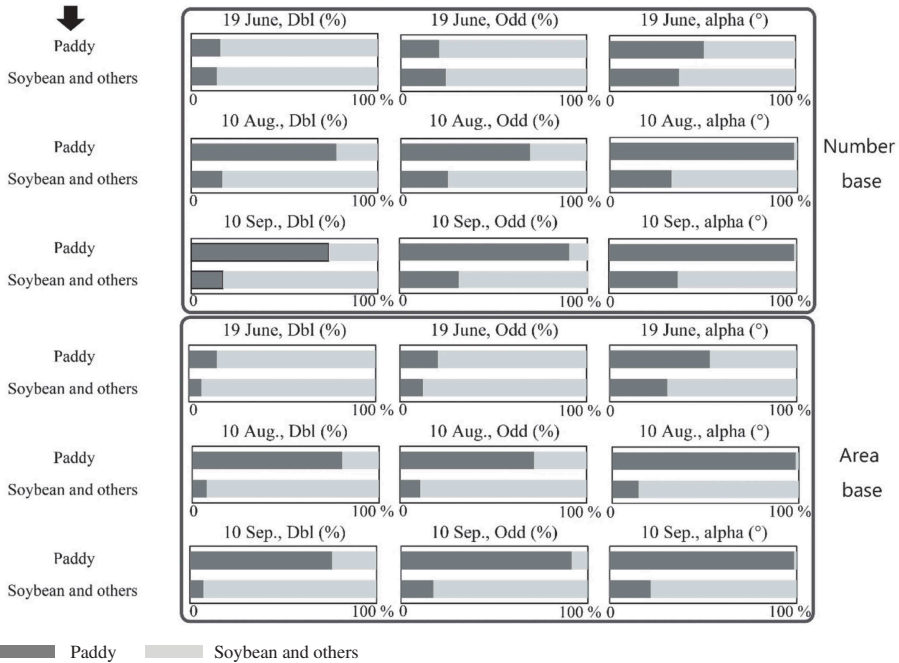|	Threshold value		
Date	Dbl (%)	Odd (%)	alpha (°)
19 June 2012	32.9	60.2	34.9
10 August 2012	33.4	48.4	36.2
10 September 2012	31.6	54.8	36.4
10 June 2013	27.7	59.9	36.9
8 August 2013	34.7	48.4	43.9
11 September 2013	37.1	50.2	43.4
12 June 2014	31.0	62.3	35.2
6 August 2014	37.7	50.5	38.3
11 September 2014	33.5	50.6	38.5

Figure 10. Charts showing cross-tabulation results for comparison of paddy rice field numbers and areas using data from optical sensor data analysis. The decomposition components of the polarimetric SAR data for 2012, obtained using threshold analysis, are also shown. The dark grey parts show the percentages of paddy rice fields and the light grey parts show the percentages of soybean and other fields based on optical sensor classification. Dbl and Odd refer to the double bounce scattering and surface scattering components, respectively. The threshold values were obtained using the method described by Otsu (1979).

The total percentage of the classification result consistency using optical sensor data and polarimetric decomposition components is shown in Table 5. The percentage agreement computed for the areal estimates is slightly larger than that of the number of fields for all periods considered in this study. Corresponding to the double bounce scattering component ratio, more than 80% of the number of agricultural parcels are consistent with optical sensor classification results on 10 August 2012, 8 August 2013, 11 September 2013, and 6 August 2014. Approximately 92% agreement in area is found for the double bounce scattering component ratio data obtained in August 2013. In addition, better than 80% agreement in area is found for the surface scattering component ratio data obtained on 10 August and 10 September 2012, 8 August and 11 September 2013, and 6 August 2014. Further, when using the alpha angle for analysis, all August and September observation data show better than 80% agreement in area with the classification results using optical sensor data.

4. Conclusions

Fully polarimetric SAR single observation has strong potential for use in paddy rice field extraction and mapping. A simple threshold analysis can also be applied to extract paddy
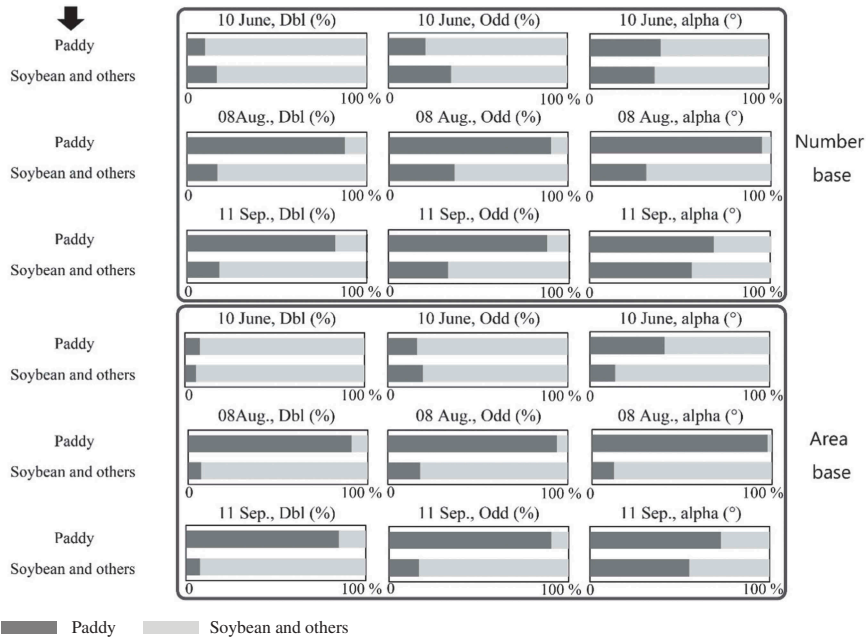
Classified by Optical Sensor

Figure 11. Charts showing cross-tabulation results for comparison of paddy rice field numbers and areas using data derived from optical sensor data analysis. The decomposition components of the polarimetric SAR data, obtained in 2013, using threshold analysis, are also shown. The dark grey parts show the percentages of paddy rice fields and the light grey parts show the percentages of soybean and other fields based on optical sensor classification. Dbl and Odd refer to the double bounce scattering and surface scattering components, respectively. The threshold values were obtained using the method described by Otsu (1979).

rice after the rice heading season in areas where the surrounding crop features are different from the paddy rice (i.e., the surrounding crop is not vertical with respect to the ground). The most suitable observation time is early August, which coincides with the rice heading season in this study. We showed that SAR detects changes in vegetation features as a direct result of the variation in scattering mechanisms over time. We also defined the relationship between the different paddy rice growth stages and the associated effects on polarimetric decomposition parameters. The useful polarimetric decomposition parameters are the double bounce and surface scattering components and the alpha angle. Extracting paddy rice fields from those of other crops with similar features (e.g. corn, wheat) is the next logical step in research on the use of fully polarimetric SAR to monitor agricultural areas.

The results of this study indicate the appropriate season for paddy rice field extraction using fully polarimetric L-band SAR. Knowledge of the suitable observation period for paddy rice field area estimation is important for planning observation programs involving spaceborne L-band SAR systems. ALOS-4 with PALSAR-3, the successor to ALOS-2, will be launched in 2020 and paddy rice field extraction and mapping will be a likely task for this and other SAR systems launched in the future.
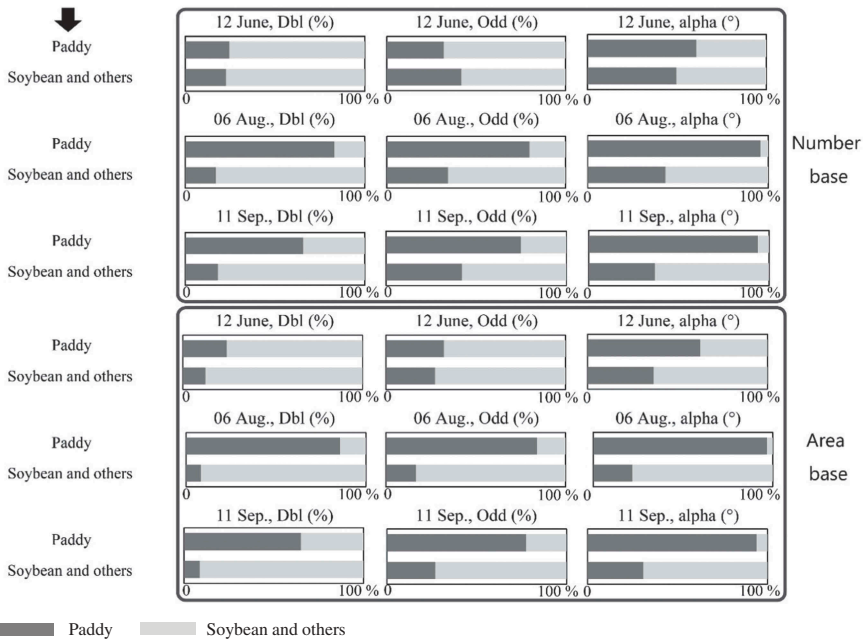
Figure 12. Charts showing cross-tabulation results for comparison of paddy rice field numbers and areas using data derived from optical sensor data analysis. The decomposition components of the polarimetric SAR data, obtained in 2014, using threshold analysis, are also shown. The dark grey parts show the percentages of paddy rice fields and the light grey parts show the percentages of soybean and other fields, based on optical sensor classification. Dbl and Odd refer to the double bounce scattering and surface scattering components, respectively. Threshold values were obtained using the method described by Otsu (1979).

Table 5. Percentage of threshold classification results using polarimetric decomposition parameters consistent with the analysis results of optical sensor data (reference data) based on agricultural parcel number and area (ha). Dbl and Odd refer to double bounce scattering and scattering components, respectively.

	Number			Area (ha)		
Date	Dbl (%)	Odd (%)	alpha (°)	Dbl (%)	Odd (%)	alpha (°)
19 June 2012	58.4	54.1	57.9	59.2	58.4	62.4
10 August 2012	81.2	72.6	79.4	86.9	81.5	91.2
10 September 2012	79.3	77.2	77.2	85.5	86.5	87.1
10 June 2013	44.3	41.4	50.9	41.1	44.2	58.6
8 August 2013	85.7	77.9	83.0	91.7	89.4	93.8
11 September 2013	82.3	78.1	56.9	87.8	87.7	62.0
12 June 2014	50.6	44.9	55.6	49.1	48.2	62.9
6 August 2014	83.1	72.9	76.5	88.0	83.9	89.5
11 September 2014	73.5	66.6	77.1	75.3	75.6	84.2

Acknowledgements

300

(ALOS 5th-RA-2048). ASTER-VA images were courtesy of NASA/METI/AIST/Japan Spacesystems, and the U.S./Japan ASTER Science Team. Landsat 7 and 8 data were courtesy of the U.S. Geological Survey.   305

Disclosure statement

Q2   No potential conflict of interest was reported by the authors.

References

Arii, M., H. Yamada, T. Kobayashi, S. Kojima, T. Umehara, T. Komatsu, and T. Nishimura. 2017. "Theoretical Characterization of X-Band Multiincidence Angle and Multipolarimetric SAR Data from Rice Paddies at Late Vegetative Stage." *IEEE Transactions on Geoscience and Remote Sensing* 55 (5): 2706–2715. doi:10.1109/TGRS.2017.2652447.

Q3

Arii, M., H. Yamada, and M. Ohki. 2018. "Characterization of L-Band MIMP SAR Data from Rice Paddies at Late Vegetative Stage." *IEEE Transactions on Geoscience and Remote Sensing* 56 (7): 3852–3860. doi:10.1109/TGRS.2018.2814996.

Cloude, S. R., and E. Pottier. 1996. "A Review of Target Decomposition Theorems in Radar Polarimetry." *IEEE Transactions on Geoscience and Remote Sensing* 34 (2): 498–518. doi:10.1109/36.485127.

Cloude, S. R., and E. Pottier. 1997. "An Entropy Based Classification Scheme for Land Applications of Polarimetric SAR." *IEEE Transactions on Geoscience and Remote Sensing* 35 (1): 68–78. doi:10.1109/36.551935.

Durden, S. L., J. J. van Zyl, and H. A. Zebker. 1989. "Modeling and Observation of the Radar Polarization Signature of Forested Areas." *IEEE Transactions on Geoscience and Remote Sensing* 27 (3): 290–301. doi:10.1109/36.17670.

Hoekman, D. H., M. A. M. Vissers, and T. N. Tran. 2011. "Unsupervised Full-Polarimetric SAR Data Segmentation as a Tool for Classification of Agricultural Areas." *IEEE Journal of Selected Topics in Applied Earth Observations and Remote Sensing* 4 (2): 402–411. doi:10.1109/JSTARS.2010.2042280.

Jiao, X., J. M. Kovacs, J. Shang, H. McNairn, D. Walters, B. Ma, and X. Geng. 2014. "Object-Oriented Crop Mapping and Monitoring Using Multi-Temporal Polarimetric RADARSAT-2 Data." *ISPRS Journal of Photogrammetry and Remote Sensing* 96 (October): 38–46. doi:10.1016/j.isprsjprs.2014.06.014.

Kurosu, T., M. Fujita, and K. Chiba. 1995. "Monitoring of Rice Crop Growth from Space Using the ERS-1 C-Band SAR." *IEEE Transactions on Geoscience and Remote Sensing* 33 (4): 1092–1096. doi:10.1109/36.406698.

Li, K., B. Brian, Y. Shao, and R. Touzi. 2012. "Polarimetric Decomposition with RADARSAT-2 for Rice Mapping and Monitoring." *Canadian Journal of Remote Sensing* 38 (2): 169–179. doi:10.5589/m12-024.

Lopez-Sanchez, J. M., F. Vicente-Guijalba, J. D. Ballester-Berman, and S. R. Cloude. 2014. "Polarimetric Response of Rice Fields at C-Band: Analysis and Phenology Retrieval." *IEEE Transactions on Geoscience and Remote Sensing* 52 (5): 2977–2993. doi:10.1109/TGRS.2013.2268319.

McNairn, H., J. Shang, X. Jiao, and C. Champagne. 2009. "The Contribution of ALOS PALSAR Multipolarization and Polarimetric Data to Crop Classification." *IEEE Transactions on Geoscience and Remote Sensing* 47 (12): 3981–3992. doi:10.1109/TGRS.2009.2026052.

Muthukumarasamy, I., R. S. Shanmugam, and S. R. Kolanuvada. 2017. "SAR Polarimetric Decomposition with ALOS PALSAR-1 for Agricultural Land and Other Land Use/Cover Classification: Case Study in Rajasthan, India." *Environmental Earth Sciences* 76: 13. doi:10.1007/s12665-017-6783-6.

Oh, Y., S. Hong, Y. Kim, J. Hong, and Y. Kim. 2009. "Polarimetric Backscattering Coefficients of Flooded Rice Fields at L- and C-Bands: Measurements, Modeling, and Data Analysis." *IEEE Transactions on Geoscience and Remote Sensing* 47 (8): 2714–2721. doi:10.1109/TGRS.2009.2014053.

Osawa, K., E. Kunii, and G. Saito. 2010. "Classification of Arable Land Using Multi-temporal Terra/ ASTER Data." *The Journal of the Japanese Agricultural Systems Society* 26 (2): 67–77. (in Japanese with English abstract). doi:10.14962/jass.26.2_67.

Otsu, N. 1979. "A Tlreshold Selection Method from Gray-Level Histograms." *IEEE Transactions on Systems, Man, and Cybernetics* 9: 62–66.

Ouchi, K., H. Wang, N. Ishitsuka, G. Saito, and K. Mohri. 2006. "On the Bragg Scattering Observed in L-band Synthetic Aperture Radar Images of Flooded Rice Fields." *IEICE Trans. Commun.* E89–B (8): 2218–2225.   355

Pottier, E., and L. Ferro-Famil 2012. "PolSARPro V5.0: An ESA Educational Toolbox Used for Self-Education in the Field of POLSAR and POL-INSAR Data Analysis". Proceedings of 2012 IEEE International Geoscience and Remote Sensing Symposium, 7377–7380. doi: 10.1109/IGARSS.2012.6351925.

Rosenqvist, A., T. Ogawa, M. Shimada, and T. Igarashi 2001. "Oniting the ALOS Kyoto Amp; Carbon   360 Initiative". In IGARSS 2001. Scanning the Present and Resolving the Future. Proceedings. Proceedings of 2001 IEEE International Geoscience and Remote Sensing Symposium (Cat. No.01CH37217), 1, 546–548 vol. 1. doi: 10.1109/IGARSS.2001.976217.

Shimada, M., N. Kawano, M. Watanabe, T. Motooka, and M. Ohki 2013b. "Calibration and Validation of the Pi-SAR-L2". In Conference Proceedings of 2013 Asia-Pacific Conference on Synthetic   365 Aperture Radar (APSAR), 194–197.

Shimada, M., M. Watanabe, T. Motooka, and Y. Kankaku 2013a. "PALSAR-2 Polarimetric Performance and the Simulation Study Using the PI-SAR-L2". Proceedings of 2013 IEEE International Geoscience and Remote Sensing Symposium - IGARSS, 2309–2312. doi:10.1109/IGARSS.2013.6723280.

Weichelt, H., W. Herr, H. Barsch, S. Itzerott, and V. Torres. 1991. "Investigation of Bioproductivity in   370 Tropical Agricultural Areas Using Remote Sensing Methods." *Acta Astronautica, International Astronautical Federation Congress* 24 (January): 93–103.

Xie, L., H. Zhang, F. Wu, C. Wang, and B. Zhang. 2015. "Capability of Rice Mapping Using Hybrid Polarimetric SAR Data." *IEEE Journal of Selected Topics in Applied Earth Observations and Remote Sensing* 8 (8): 3812–3822. doi:10.1109/JSTARS.2014.2387214.   375

Yamaguchi, Y., T. Moriyama, M. Ishido, and H. Yamada. 2005. "Four-Component Scattering Model for Polarimetric SAR Image Decomposition." *IEEE Transactions on Geoscience and Remote Sensing* 43 (8): 1699–1706. doi:10.1109/TGRS.2005.852084.

Yang, H., G. Yang, R. Gaulton, C. Zhao, Z. Li, J. Taylor, D. Wicks, A. Minchella, E. Chen, and X. Yang. 2018. "In-Season Biomass Estimation of Oilseed Rape (Brassica Napus L.) Using Fully Polarimetric   380 SAR Imagery." *Precision Agriculture* 1–19. doi:10.1007/s11119-018-9587-0.

Yonezawa, C. 2017. "Possibility of Well Grown Paddy Rice Field Identification Using PALSAR-2 Full Polarimetric Data." *Journal of the Remote Sensing Society of Japan* (in Japanese with English abstract) 37 (3): 204–212. doi:10.11440/rssj.37.204.

Yonezawa, C. 2018. "Paddy Rice Field Extraction Using ALOS-2 Palsar-2 Full Polarimetric Data with   385 Agricultural Parcel Vector Data". Proceedings of 2018 IEEE International Geoscience and Remote Sensing Symposium - IGARSS.

Yonezawa, C., M. Negishi, K. Azuma, M. Watanabe, N. Ishitsuka, S. Ogawa, and G. Saito. 2012. "Growth Monitoring and Classification of Rice Fields Using Multitemporal RADARSAT-2 Full-Polarimetric Data." *International Journal of Remote Sensing* 33 (18): 5696–5711. doi:10.1080/01431161.2012.665194.   390

Yonezawa, C., and M. Watanabe 2015. "Agricultural Field Observation by Space and Airborne Polarimetric L-Band SAR Data". Proceedings of 2015 IEEE International Geoscience and Remote Sensing Symposium (IGARSS), 3985–3988. doi: 10.1109/IGARSS.2015.7326698.